06

# Electrophysical properties of different types of shungite rocks

© I.A. Moshnikov, V.V. Kovalevski

Institute of Geology, Karelian Research Center, Russian Academy of Sciences,

185910 Petrozavodsk, Russia e-mail: kovalevs@krc.karelia.ru

Received December 12, 2024 Revised April 14, 2025 Accepted April 28, 2025

Two types of shungite rocks with different chemical and mineralogical compositions, initial and modified, were studied. During heat treatment, nanoscale hollow carbon structures, fibrous silicon carbides, micro-sized iron silicide particles, and glassy microspheres were formed in the modified samples. The electrical conductivity of these samples at temperatures between 77 and 300 K and shielding effectiveness at frequencies from 100 kHz to 1 GHz were measured. The initial and modified samples exhibited a semiconductor type of conductivity, with activation energies ranging from 0.0007 to 0.0086 eV. The electrical conductivity and shielding effectiveness of the modified shungite samples can increase or decrease depending on the type and composition of the rock.

Keywords: Shungite rock, heat treatment, electron microscopy, Raman spectroscopy, electrical conductivity, shielding effectiveness.

DOI: 10.61011/TP.2025.08.61737.457-24

## Introduction

Shungite rocks (SR) are ancient (the age is about 2 billion years) carbon-bearing volcanogenic sedimentary rocks of Karelia, which are unique in terms of formation conditions, commercial reserves (more than 4 billion tons) and a structure and properties of carbonaceous matter (shungite). The shungite rocks substantially differ both in percentage of shungite (from 1% to more than 98%) and chemical and mineralogical compositions. According to permolecular, molecular and band structures, shungite can be characterized as natural nanostructured fullerenelike carbon with typical physical and chemical properties [1,2]. Technologically, shungite rock is a carbon-mineral composite with micro- and nano-dispersed distribution of the components. Structure-morphology specific features of shungite and mineral components and their percentage determine various fields of practical application of shungite rock [3]. At the same time, a structural state, composition and physical-chemical properties of shungite and shungite rock can substantially vary under effect of various methods of modification, for example, during thermal sputtering [4] as well as under thermal and chemical impact [5]. Most drastically, the shungite rocks are transformed during high-temperature treatment in a reducing atmosphere to form nanoscale carbon and ceramic components that have promising physical-chemical properties [6].

Decisive properties of the carbon materials (CM) to be used in high-tech fields of application are their electrophysical properties, which depend on a form, size and structure of the carbon materials [7,8]. In particular, the electrophysical properties are directly related to one of the most demanded fields of practical application of the carbon materials as materials that ensure safety of human

life from natural and man-made electromagnetic radiation (EMR). It is noted in the literature that in the last few decades a level of man-made electromagnetic background has increased in tens of thousand times to pose a danger for human life and health [9,10]. Generally, the materials used for EMR protection can be classified depending on a type of a binder, a filler and structural characteristics. At the same time, the more effective are mixed fillers that contain conductive components (powders, fibers, films), magnetic fillers (ferrites), disperse semiconductors (oxides, sulfides, carbides of metal and silicon) and dielectrics that provide various mechanisms of EMR scattering within the wide frequency range [11]. It is also promising to use nanostructured fillers, for which interaction with EMR is determined by parameters of nanoparticles and a nature of their distribution in the composite with respective changes of the electrophysical properties [12]. Being a natural carbon material, shungite has several structural specific features that affect its electrophysical properties. For example, at low currents, the type of conductivity of shungite depends on intercalation of the elements on boundaries of the graphene layers [13]. It was also found that unlike other natural carbons the structurally-anisotropic shungites exhibited the Meissner effect and increase of diamagnetism within the range 90-150 K, which is typical for doped fullerites [1]. At the same time, some studies note that shungite-filled composites are promising materials for protection of biological objects and equipment against EMR within the wide frequency range [14,15].

The aim of this study is to investigate the electrophysical properties of the initial and modified shungite rocks of a various type for designing effective electromagnetic field (EMF) shielding materials.

Shungite rock	C*	Chemical composition (in oxides)											
		SiO <sub>2</sub>	TiO <sub>2</sub>	Al <sub>2</sub> O <sub>3</sub>	Fe <sub>2</sub> O <sub>3</sub>	MnO	MgO	CaO	Na <sub>2</sub> O	K <sub>2</sub> O	S	ACL*	
ShRL	42	39	0.51	7.12	5.54	0.023	1.44	0.13	3.09	0.42	0.16	42.4	
ShRL/HT	36	42.4	0.54	7.71	5.87	0.028	1.67	0.20	3.42	0.45	0.28	36	
ShRMr	41	46.5	0.36	4.51	2.74	0.017	0.45	0.51	< 0.01	1.81	0.34	43.6	
ShRMr/HT	32	53.1	0.41	5.11	3.17	0.019	1.65	0.80	< 0.01	2.07	0.53	32	

**Table 1.** Chemical composition (wt.%) of the initial (ShRL and ShRMr) and heat-treated (ShRL/HT and ShRMr/HT) rocks as per results of X-ray fluorescence analysis

Note. \*C — the carbon content is determined by results of derivatographic analysis; \*\*ACL — losses during calcination in air (1000 °C, 30 min) from release of CO<sub>2</sub> with oxidation of carbon and decomposition of carbonates.

## **Experiment**

Comparative investigation was for two basic types of shungite rocks with the carbon content  $\sim 40\%$ , which belong to the second (the Lebeschina region — ShRL) and sixth (the Mironovskaya region - ShRMr) shungitebearing stratum and are characterized by various P-Tconditions and rock age [3] and a various chemical composition as well (Table 1). The ShRL sample as per the ratio Na/K > 1 belongs to the sodium type of the shungite rock, while the ShRMr sample when Na/K < 1 belongs to the sodium type of the shungite rock. The shungite rock powders of a fraction of below 0.1 mm were used for modification and investigation. Heat treatment (HT) was carried out at the temperature of 1600 °C for 10 min in the VUP-5 installation in the argon atmosphere at the heating rate of about 1000 °C/min. temperature was measured using a fiber-optic pyrometer PD-7-02 ( $T_{\rm max}$  — 2500 °C, the error is  $\pm 0.5$  %). The mineralogical composition of the initial and modified rocks was determined by means of X-ray diffraction analysis in the ARL X'TRA diffractometer using the Siroquant software. The structural state of shungite carbon before and after heat treatment was evaluated by Raman scattering spectra using the dispersion Raman spectrometer Nicolet Almega XR with the green laser (532 nm, Nd-YAG). In order to study a morphology of micro-sized components and to determine their microelement composition, we have used a scanning electron microscope (SEM) VEGA 11 LSH that was produced by Tescan and equipped with an energy-dispersive unit INCA Energy produced by Oxford The morphology and the structural state Instruments. of the nanoscale components of shungite rock after heat treatment was detected by means of transmission electron microscopy (TEM) and selected area electron diffraction (SAED) on ethanol-dispersed powders which were placed on standard copper meshes in the electron microscope EM-125.

EMF shielding properties were quantitatively evaluated by using shielding effectiveness in decibels [16]. Conductivity and SE were measured on the powders. Before the measurement, the powders were pressed in a coaxial measurement cell by the force of 150 kgf. Conductivity was measured at the temperatures from 77 to 300 K using a coaxial transmission line and a universal meter LCR E7-8 at the frequency of 1kHz in a two-contact method. The measurement line was cooled by liquid nitrogen. After evaporation of nitrogen, the sample temperature was increased to the room temperature by natural heat exchange with the environment for 2 h. The measurements were carried out every 2-3 °C during increase of the temperature. SE was measured at the room temperature using selective microvoltmeters SMV 8.5 and SMV 11 within the frequency range from 100 kHz to 1 GHz by the coaxial method of electromagnetic spectrum analysis, which was based on the ASTM D4935 standard for the coaxial transmission line. SE was determined by measuring signal attenuation when transmitting through the transmission line with the sample placed in the measurement

#### Results and discussion

Heat treatment caused significant changes in the composition of the initial rocks. For the shungite rock of the sodium type, which in the initial state contains carbon, quartz, albite and chlorite, heat treatment causes reduction of the carbon content and quartz with full transformation of albite and chlorite, which is accompanied by origination of significant amounts of silicon carbide, iron silicide and the amorphous phase, which are detected by Xray diffraction analysis (Table 2). For the shungite rock of the potassium series, which contains carbon, quartz and microcline, there is also formation of silicon carbide, iron silicide and the amorphous phase (Table 2). The scanning electron microscopy can visualize and determine the composition of the micro-sized components (Fig. 1, a): iron silicides as light areas on the SEM images, which have sizes of below  $1 \mu m$  and spherical formations of the complex composition (Si, Al, Mg, Na, K, O) with the sizes

**Table 2.** Mineral composition (as per results of X-ray study), the carbon parameters (as per Raman-scattering spectroscopy) and the electrophysical properties of the shungite rocks of the various type before and after heat treatment (HT)

Commercial manufacture	Sh	RL	ShRMr			
Composition, properties	Initial	HT	Initial	HT		
Mineral composition, wt.%	X-ray diffraction analysis					
Shungite* (mineraloid) — C, the impurities — sulfides, carbonates, etc. micro- and nano-minerals	42	36	41	32		
Quartz** — SiO <sub>2</sub> , the impurities Ca, Fe, Mn, Cu, Mg, etc.	16	6	48	10		
Muscovite** — KAl <sub>2</sub> (AlSi <sub>3</sub> O <sub>10</sub> )(OH) <sub>2</sub> , the impurities Mg, Fe, Cr, Mn, etc.			9.5			
Microcline** — K[AlSi <sub>3</sub> O <sub>8</sub> ], the impurities Na, Fe, Ca, Li			1.5			
Albite** — Na[AlSi <sub>3</sub> O <sub>8</sub> ], the impurities K, Ca, Rb, Cs, etc.	40					
Chlorite** — $(Mg,Fe)_3(Si,Al)_4O_{10}(OH)_2(Mg,Fe)_3(OH)_6$ , the impurities Li, Cr, Zn, Mn, etc.	2					
SiC**		26		34		
Fe <sub>3</sub> Si**		15		12		
Amorphous phase*** (Si, Al, Mg, Na, K, O)		17		12		
Carbon parameters	Raman spectroscopy					
La, nm	2.55	6.83	2.05	5.78		
Leq, nm	3.26	20.4	2.52	17.5		
$\Delta w_{ m 2D},{ m cm}^{-1}$	59	15	78	19		
Properties	Electrophysical measurements					
$\sigma$ , S/m	250	300	135	60		
$E_1$ , eV	0.0086	0.0066	0.0057	0.0028		
$E_2$ , eV	0.0007	0.0019	n/a	n/a		
SE, dB	46.9/48.1/57.3	48.6/51.3/67.3	45.0/46.3/54.5	43.2/44.2/52.6		
(0.1/100/1000 MHz)						

Note. \*C — the carbon content is determined by results of the derivatographic analysis; \*\* — the composition is calculated in the Siroquant software by the content of the crystal phases in the X-ray diffraction spectrum taking into account the known carbon content; \*\*\* — the content of the amorphous phase is evaluated based on its microelement composition, general chemical analysis and X-ray pattern background in the Siroquant software.

from fractions to  $5\,\mu m$ . Based on the X-ray diffraction analysis, the formations with such a composition are not represented by a crystal phase and can be considered as amorphous and determined as glass spheres when taking into account highly-blurred peaks on the X-ray patterns. According to the TEM results, heat treatment of the shungite rock results in origination of nanoscale hyper-fullerene (hollow spherical or ellipsoid) carbon structures, fibrous silicon carbides and iron silicide particles (Fig. 1, b, c). New nanoscale phases are formed during heat treatment in solid-state reactions, included those catalytically-initiated ones, between the mineral components and carbon of the shungite rock. Finely-globular shungite carbon is directly transformed into the hyper-fullerene structures (Fig. 1, b), which are similar to the particles detected in the shungite rock that is

heated as a result of contact metamorphism [17]. Interaction of carbon with finely-dispersed minerals results in formation of nanofibers and silicon carbide nanoparticles as well as iron silicide nanoparticles that can be encapsulated in the carbon shells (Fig. 1, b). Generally, for both the rocks, heat treatment results in formation of similar complexes of overlapping nanoscale components of a different nature (conductive, magnetic and dielectric), which can ensure effective scattering of microwave energy [11]. However, the first rock has (Table 2) higher determined contents of carbon and ferromagnetic silicide Fe<sub>3</sub>Si that has a higher coefficient of spin polarization of electrons [18], while the second rock has a higher determined content of silicon carbide that is characterized by minimum values of dielectric losses [19].

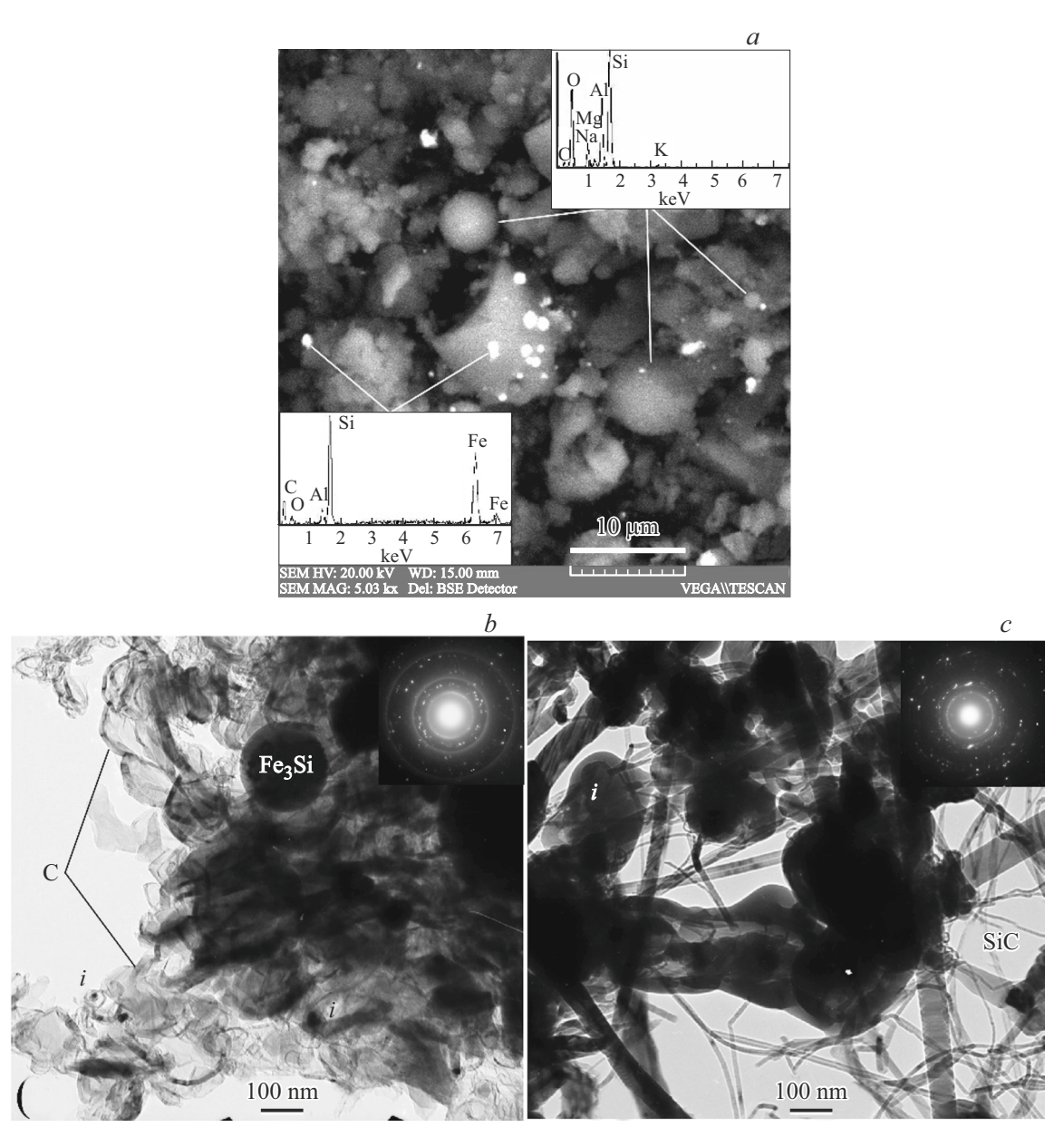


Figure 1. a — the SEM image of micro-sized components of the heat-treated shungite rocks in back-scattered electrons and their energy-dispersive spectra; b, c — the TEM images and their respective SAED patterns (in the inserts) of hyper-fullerene carbon structures, nanoscale iron silicide particles, including those encapsulated in carbon shells (marked by i), and of silicon carbide fibers.

The structural state of shungite carbon was evaluated by the Raman scattering spectra (Fig. 2). In comparison with carbon of the ShRMr shungite rock, carbon of the ShRL initial sample is characterized by an increased size of the non-defect area of the graphene layer, which is identical to the coherent scattering area (La) as per X-ray data. It also has higher three-dimensional ordering as per FWHM 2D  $(\Delta w_{\rm 2D} \sim 2690\,{\rm cm}^{-1})$  [20]. At the same time, an increased length of the continuous graphene layer with taking into account tortuosity (Leq) indicates a higher free path length of phonons and electrons in the layer [20] (Table 2). Heat treatment of both the shungite rocks causes formation of shallow carbon structures and increase of general ordering of carbon, which is indicated by higher values of Leq and lower values of  $\Delta w_{2D}$  (Table 2). However, carbon of the ShRL sample has higher sizes of the graphene layer and higher three-dimensional ordering, thereby determining its higher conductivity.

The measured values of conductivity of the initial samples significantly differ despite the similar carbon content (Table 2). At the same time, higher conductivity of the ShRL sample in relation to ShRMr complies with respectively higher ordering of carbon. Heat treatment results in reduction of the carbon content in both the samples. However, despite it, conductivity of the ShRL sample increases, while that of ShRMr decreases (Table 2). The dependence of

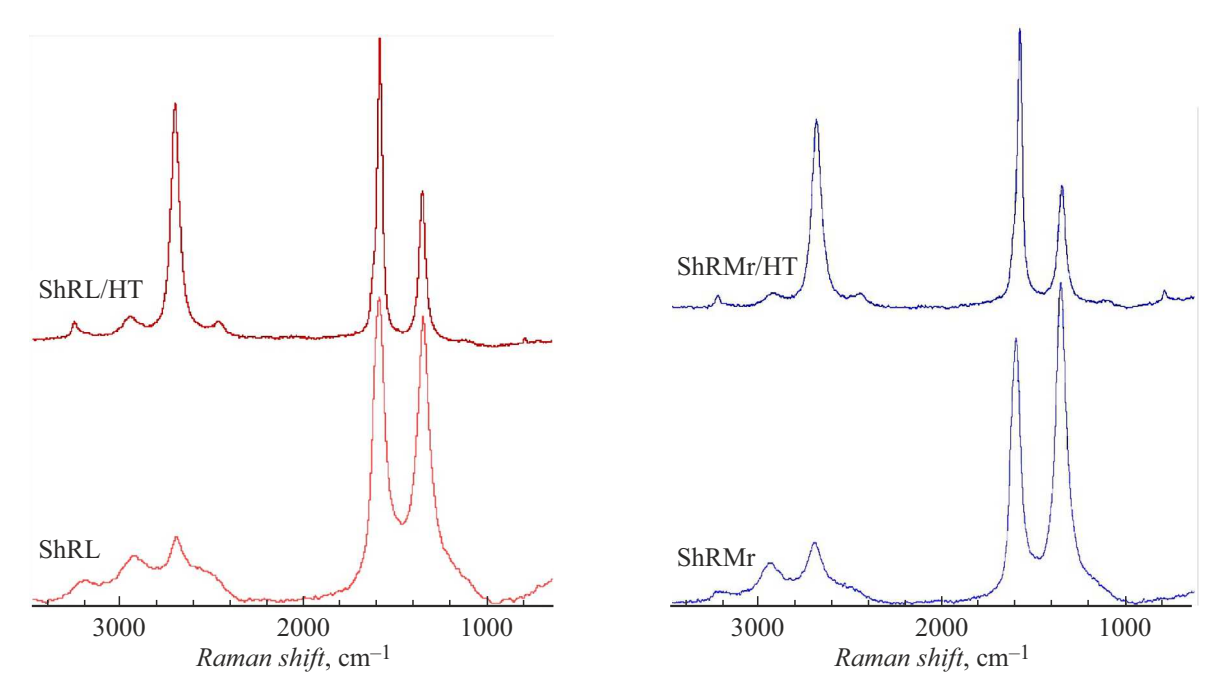
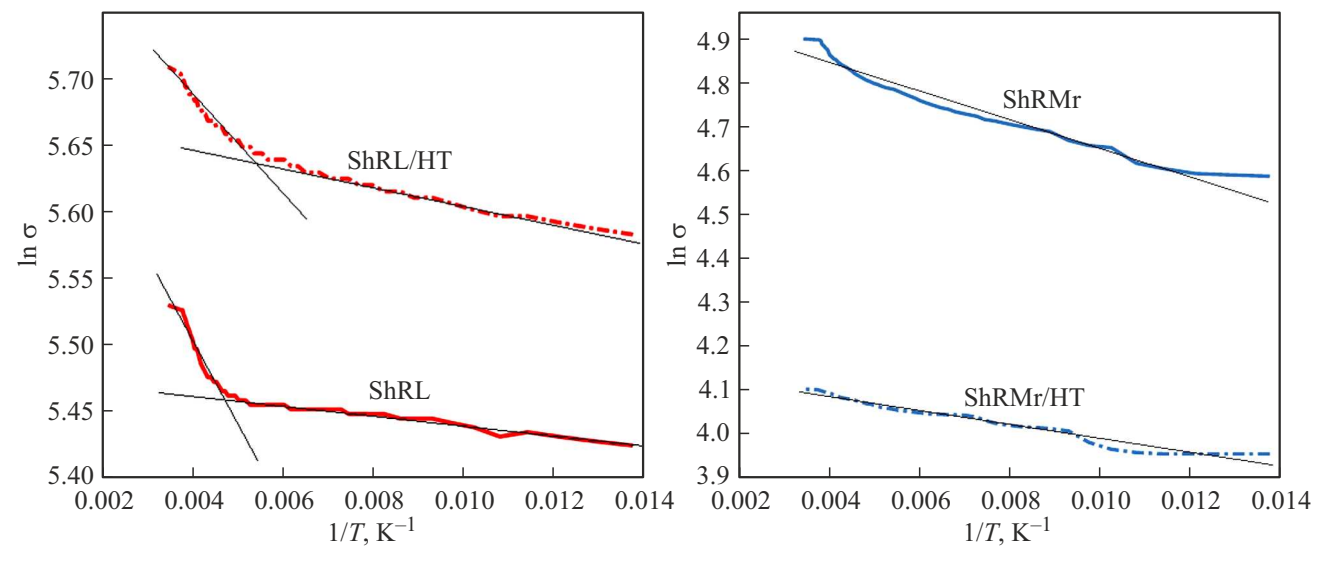


Figure 2. Spectra of Raman scattering of the initial (ShRL and ShRMr) and heat-treated (ShRL/HT and ShRMr/HT) samples.



**Figure 3.** Graphs of the dependence of conductivity on the temperature for the initial (ShRL and ShRMr) and heat-treated (ShRL/HT and ShRMr/HT) samples in a semilogarithmic scale.

conductivity on the temperature for the shungite rock of the different type has a semiconductor nature of conductivity within the range from 77 to 300 K both before and after heat treatment. Based on the obtained results, the energy of activation of conductivity of the samples was evaluated by plotting a dependence of conductivity on the temperature in the semilogarithmic system of coordinates [21]. If the ordinate axis has  $\ln \sigma$  and the abscissa axis has 1/T, then the energy of activation can be calculated as  $E=2k \lg \alpha$ , where  $\alpha$ — a slope of the straight line to the abscissa axis, k— the Boltzmann constant. The value of

the energy of activation of conductivity is a combination of the energy of activation of charge-carrier generation processes and their movement. Generally, this dependence is described by a broken line with an inflection point at the temperature of transition between different types of conductivity [22]. tg  $\alpha$  was calculated by approximation of the obtained curves by means of a linear type of regression (Fig. 3). The coefficient of determination for the ShRMr and ShRMr/HT samples turned out to be 0.94 and 0.97, and 0.61 and 0.85 for the ShRL and ShRL/HT samples, respectively.

The quite high values of the coefficient of determination for the ShRMr and ShRMr/HT samples made it possible to evaluate  $\operatorname{tg} \alpha$  and E for each of the respective curves (Fig. 3, Table 2). On the contrary, the low values of the coefficient of determination for ShRL and ShRL/HT, which indicate significant inflection of the curves, enabled their division into two portions, wherein each of them was well approximated by linear regression with the coefficient of determination of above 0.9 (Fig. 3, Table 2). Two values of  $tg \alpha$  and E have been determined for each of these samples. Presence of inflection of the graphs of the dependence of conductivity on the temperature for the ShRL and ShRL/HT samples indicates that at 180 and 200 K, respectively, there is increase of the energy of activation without the change of the semiconductor nature of conductivity. However, despite selection of the linear regression for the ShRMr and ShRMr/HT samples, the portions of the curves from 80 K (0.012 along 1/T in Fig. 3) to 110 K (0.009) also exhibit the inflection, thereby indicating the local change of the energy of activation for these samples. Thus, for both the rocks after heat treatment the values of the energy of activation of conductivity are reduced, while their typical specific features are preserved.

It has been previously found that the energy of activation of conductivity of the shungite rock did not depend on the carbon content and was within the range 0.003-0.005 eV in the interval of relatively low temperatures (up to 300 K) [23]. The values of the energy of activation of conductivity, which are obtained in our study, are close to these data, but with the similar carbon percentage they depend on the rock type and its transformation during heat treatment. The materials obtained after heat treatment of both the shungite rocks are complex multiphase composites that contain, in addition to carbon, iron silicide that has high energy of activation of conductivity (at least 0.015 eV) [24]. At the same time, the typical specific features of the obtained dependences (Fig. 3) are still similar both for the initial and heat-treated rocks, in which the only chemically-unchanged component is still carbon, thereby making it possible to conclude that it predominantly affects conductivity of the samples.

The shielding effectiveness (SE) at the room temperature within the frequency range from 100 kHz to 1 GHz increases with the frequency for all the sample, although it is different for ShRL and ShRMr as shown in Fig. 4 and in Table 2. SE increase is natural, since decay of the electromagnetic wave in the shield functionally depends on specific conductivity of the material, which, in turn, increases with increase of the frequency. In terms of wave representations, the shielding effect is manifested due to multiple reflections of the electromagnetic waves from the shield surface and decay of the electromagnetic energy in its thickness. Heat treatment and accompanying transformation of the rock result in a different degree of reduction of the carbon percentage as well as formation of nanoscale iron silicides and silicon carbides. The differences in the content of these components cause multidirectional changes

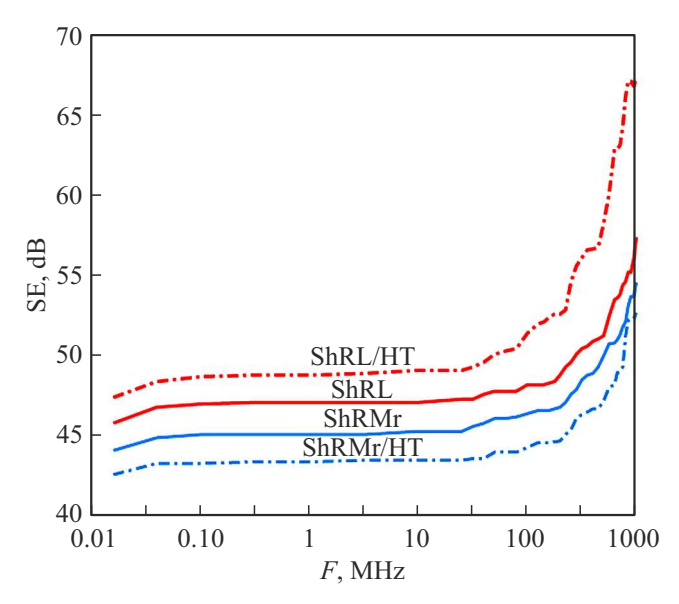


**Figure 4.** Graphs of the dependence of shielding effectiveness (SE) on the frequency of the electromagnetic field for the initial and heat-treated shungite rocks.

of the shielding effectiveness of the obtained materials and comply with a change of their conductivity (Table 2). For ShRL/HT, the shielding efficiency increases, while for ShRMr/HT it decreases. Since SE is a function of both reflection and absorption of EMR by the material [25], then for the heat-treated rocks SE is determined both by their conductivity as well as magnetic losses due to natural ferromagnetic resonance and vortex currents in iron silicide and dielectric losses by varying permittivity and polarization relaxation in carbon and silicon carbide [26]. Additionally, attenuation of radiation can be caused not only by dielectric losses, but multiple reflection of the electromagnetic wave within an area of significant change of wave resistance. These conditions can originate both inside the hollow carbon structures and on the surface of metal-containing inclusions.

Based on significant drop of conductivity for the ShRMr/HT sample (Table 2), it follows that the main factor of SE change is conductivity of the rock, which is related to distribution and conductivity of carbon, silicon carbide and iron silicide that are contained therein. Generally, the electrophysical properties of the shungite rock are caused by structural specific features of the carbon and mineral components, their distribution in the rock and presence of microelements and minerals that have magnetic and dielectric properties. A variety of the shungite rocks makes it possible to vary their composition and properties within a wide range by modification and to create composites that combine components which cause electromagnetic and dielectric EMR losses, which is an important field in designing effective EMF shielding materials [26].

### **Conclusions**

We have studied the shungite rocks of the various type with the same percentage of carbon, but a different mineral composition and ordering of carbon. The shungite rocks were subjected to high-temperature treatment that caused formation of the nanoscale hollow carbon structures, the fibrous silicon carbides, the iron silicide particles and the glass microspheres. It is found that the electrophysical properties of the initial and heat-treated shungite rocks are determined by the content and ordering of carbon as well as mineral components and can significantly differ for the shungite rocks with the similar carbon content. The conductivity of the shungite rock at the temperatures from 77 to 300 K has the semiconductor nature of conductivity, but a different form due to the different energy of activation of conductivity (0.0007-0.0086 eV) and its change with the temperature for the initial and heat-treated rocks. The shielding effectiveness is measured at the room temperature within the frequency range from 100 kHz to 1 GHz and it is found that heat treatment results in opposite changes in the shielding effectiveness: its increase for the shungite rock of the sodium type and decrease for the shungite rock of the potassium type. As a result of the performed studies, it is found that for effective use of the shungite rocks as EMF shielding materials it is necessary to take into account not only the carbon content, but its structural state and the rock type that determines its mineral composition.

#### **Acknowledgments**

The authors would like to thank Yu.A. Markovskii for heat treatment and I.S. Inina for X-ray diffraction analysis of the shungite rocks as well as reviewers for their critical comments.

#### **Funding**

The study was carried out under the state assignment ( $N_0$ 1022040400163-5) as per the scientific research plan GI of KarRC RAS using the equipment of Collective Use Center of KarRC RAS.

## Conflict of interest

The authors declare that they have no conflict of interest.

#### References

- [1] V.V. Kovalevski, A.V. Prikhodko, P.R. Buseck. Carbon, 43 (2), 401 (2005). DOI: 10.1016/j.carbon.2004.09.030
- [2] M.A. Augustyniak-Jablokow, Y.V. Yablokov, B. Andrzejewski, W. Kempinski, S. Los, K. Tadyszak, M.Y. Yablokov, V.A. Zhikharev. Phys. Chem. Minerals, 37 (4), 237 (2010). DOI: 10.1007/s00269-009-0328-9
- [3] Yu.E. Deines, V.V. Kovalevskii, I.V. Kochneva, I.A. Moshnikov, V.S. Rozhkova, Tr. KarNTs, 2, 84 (2020) (in Russian). DOI: 10.17076/geo1187

- [4] I.A. Moshnikov, V.V. Kovalevski, Yu.A. Markovskii. Fullerenes, Nanotubes and Carbon Nanostructures, 30 (1), 1 (2021). DOI: 10.1080/1536383X.2021.1998004.
- V.V. Kovalevski, I.V. Kochneva, V.S. Rozhkova. Inorganic Mater., 59 (7), 736 (2023).
   DOI: 10.1134/s0020168523070099.
- [6] S.V. Kovalevskii, I.A. Moshnikov, V.V. Kovalevski. Nanosyst.: Phys. Chem. Math., 9 (4), 468 (2018).
   DOI: 10.17586/2220-8054-2018-9-4-468-472
- [7] G.V. Simbirtseva, N.P. Piven', S.D. Babenko. Russ. J. Phys. Chem. B, 14 (6), 980 (2020).
   DOI: 10.1134/S1990793120060287.
- [8] S.P. Belyaev, S.K. Gordeev, V.A. Chekanov, I.V. Golosovsky,
   S.K. Gordeev, S.B. Korchagina, I.A. Denisov, P.I. Belobrov.
   Physics Solid State, 56 (1), 152 (2014).
   DOI: 10.1134/S1063783414010028
- [9] H. Akbari, Sh. Taeb, A. Adibzadeh, H. Akbari. J. Biomed. Phys. Eng., 13 (4), 299 (2023).
   DOI: 10.31661/jbpe.v0i0.2010-1203
- [10] S. Kumar, P.P. Pathak. Int. J. Innov. Sci. Res. Technol., 9 (3), 2008 (2024). DOI: 10.38124/ijisrt/IJISRT24MAR1491
- [11] M.F. Elmahaishi, R.S. Azis, I. Ismail, F.D. Muhammad. J. Mater. Res. Techn., 20, 2188 (2022). DOI: 10.1016/j.jmrt.2022.07.140.
- [12] E.I. Terukov, A.A. Babaev, A.G. Tkachev, D.V. Zhilina. Tech. Phys., 63 (7), 1044 (2018).
   DOI: 10.1134/S1063784218070289
- [13] E.A. Golubev. Physics Solid State, **55** (5), 1078 (2013). DOI: 10.1134/S1063783413050107
- [14] Yu.V. Samukhina, G.M. Nikoladze, T.A. Kulkova,
   A.K. Buryak. Russ. J. Phys. Chem. A, 97 (2), 373 (2023).
   DOI: 10.1134/S0036024423020231
- [15] V.P. Podolsky, V.V. Volkov, O.B. Kukina, A.V. Andreev. Russ. J. Building Construction and Architecture, 3 (55), 7 (2022). DOI: 10.36622/VSTU.2022.55.3.007
- [16] I.A. Moshnikov, V.V. Kovalevski. Nanosyst.: Phys. Chem. Math., 7 (1), 214 (2016).
   DOI: 10.17586/2220-8054-2016-7-1-214-219
- [17] S.Y. Chazhengina, V.V. Kovalevski. Eur. J. Mineral, 25, 835 (2013). DOI: 10.1127/0935-1221/2013/0025-2327
- [18] S.A. Lyashchenko, Z.I. Popov, S.N. Varnakov, E.A. Popov, M.S. Molokeev, I.A. Yakovlev, A.A. Kuzubov, S.G. Ovchinnikov, T.S. Shamirzaev, A.V. Latyshev, A. Saranin. J. Exp. Theor. Phys., 120 (5), 886 (2015). DOI: 10.1134/S1063776115050155
- [19] B. Zhang, Q. Jing, Sh. Yan, J. Guo, W. Liu, Ch. Sun, Z. Wang. Carbon, 218 (1), 118727 (2024).
   DOI: 10.1016/j.carbon.2023.118727
- [20] N. Larouche, B.L. Stansfield. Carbon, 48 (3), 620 (2010). DOI: 10.1016/j.carbon.2009.10.002
- [21] B.L.H. Azari, T. Wicaksono, J.F. Damayanti, D.F.H. Azari. Comput. Exp. Res. Mater. Renewable Energy (CERiMRE), 4 (2), 71 (2021). DOI: 10.19184/cerimre.v4i2.28371
- [22] N.F. Mott, E.A. Davis. Electronic Processes in Non-Crystalline Materials (Clarendon Press, Oxford, 1979)
- [23] E.A. Golubev, I.V. Antonets, R.I. Korolev. FTT, 65 (12), 2111 (2023) (in Russian). DOI: 10.61011/FTT.2023.12.56735.5136k
- [24] A.A. Grebennikov, V.S. Zheleznyi, Yu.E. Kalinin, V.A. Makagonov, O.N. Pevchenko. Vestnik Voronezhskogo gos. tekh. un-ta, **9** (6–1), 77 (2013) (in Russian).
- [25] D.D.L. Chung. Carbon, **39** (2), 279 (2001). DOI: 10.1016/S0008-6223(00)00184-6
- [26] A. Xie, B. Zhang, Y. Ge, X. Wang, P. Xu, Zh. Feng, Y. Maozhong, Zh. Zhe. J. Mater. Res. Tech., 25, 4833 (2023). DOI: 10.1016/j.jmrt.2023.06.132

Translated by M.Shevelev